

Preparation of spin squeezed state in SiV centerscoupled by diamond waveguide

Yong-Hong Ma(马永红), Yuan Xu(许媛), Quan-Zhen Ding(丁全振), and Yu-Sui Chen(陈予遂)
Citation: Chin. Phys. B, 2021, 30 (**10**): 100311. DOI: 10.1088/1674-1056/ac05b3
Journal homepage: http://cpb.iphy.ac.cn; http://iopscience.iop.org/cpb

What follows is a list of articles you may be interested in

Quantum speed limit for the maximum coherent state under the squeezed environment

Kang-Ying Du(杜康英), Ya-Jie Ma(马雅洁), Shao-Xiong Wu(武少雄), and Chang-Shui Yu(于长水)
Chin. Phys. B, 2021, 30 (**9**): 090308. DOI: 10.1088/1674-1056/ac0daf

Entanglement of two distinguishable atoms in a rectangular waveguide: Linear approximation with single excitation

Jing Li(李静), Lijuan Hu(胡丽娟), Jing Lu(卢竞), and Lan Zhou(周兰)
Chin. Phys. B, 2021, 30 (**9**): 090307. DOI: 10.1088/1674-1056/ac0bb3

Preparation of a two-state mixture of ultracold fermionic atoms with balanced population subject to the unstable magnetic field

Donghao Li(李东豪), Lianghui Huang(黄良辉), Guoqi Bian(边国旗), Jie Miao(苗杰), Liangchao Chen(陈良超), Zengming Meng(孟增明), Wei Han(韩伟), and Pengjun Wang(王鹏军)
Chin. Phys. B, 2021, 30 (**9**): 090303. DOI: 10.1088/1674-1056/abee6e

Nonlocal advantage of quantum coherence and entanglement of two spins under intrinsic decoherence

Bao-Min Li(李保民), Ming-Liang Hu(胡明亮), and Heng Fan(范桁)
Chin. Phys. B, 2021, 30 (**7**): 070307. DOI: 10.1088/1674-1056/abff2a

Steered coherence and entanglement in the Heisenberg *XX* chain under twisted boundary conditions

Yu-Hang Sun(孙宇航) and Yu-Xia Xie(谢玉霞)
Chin. Phys. B, 2021, 30 (**7**): 070303. DOI: 10.1088/1674-1056/abe1a9

Preparation of spin squeezed state in SiV centers coupled by diamond waveguide*

Yong-Hong Ma(马永红)[1,†], Yuan Xu(许媛)[1], Quan-Zhen Ding(丁全振)[2], and Yu-Sui Chen(陈予遂)[3,‡]

[1] School of Science, Inner Mongolia University of Science and Technology, Baotou 014010, China
[2] Department of Physics, and Center for Quantum Science and Engineering, Stevens Institute of Technology, Hoboken, NJ 07030, USA
[3] Department of Physics, New York Institute of Technology, Old Westbury, NY 11568, USA

(Received 3 March 2021; revised manuscript received 7 April 2021; accepted manuscript online 27 May 2021)

Spin squeezing is a fascinating manifestation of many-particle entanglement and one of the most promising quantum resources. In this paper, we propose a novel realization of a solid-state quantum spin squeezing by applying SiV centers embedded in a diamond waveguide with the help of a microwave field. The phenomena about the generation of spin squeezing are analyzed numerically in Markovian environments. Our analysis shows that spin squeezing can be generated with the microwave field's help under some realistic conditions, despite the presence of dephasing and mechanical damping. This solid-state spin squeezing based on SiV centers in diamonds might be applied to magnetometers, interferometry, and other precise measurements.

Keywords: spin squeezed state, SiV center, diamond waveguide

PACS: 03.65.Yz, 61.72.jn **DOI:** 10.1088/1674-1056/ac05b3

1. Introduction

A spin squeezed state is from an ensemble of spins whose fluctuation in one collective spin direction to the mean spin direction is smaller than the classical limit.[1] As an important quantum resource, spin squeezing has many potential applications, such as quantum information, quantum measurement, quantum computing,[2,3] and quantum network.[4,5] Not only particle entanglement can be studied, but also the accuracy of quantum computation can be greatly improved by preparing the spin-squeezing state.[6,7] Thus it promotes the development of quantum information.[8]

Two types of spin squeezing called one-axis twisting model and two-axis twisting models, were provided by Kitagawa *et al.*[1] and Wineland *et al.*,[9] respectively. At present, a larger number of spin squeezing schemes were proposed with the development of quantum information, such as in Bose–Einstein condensates,[10–17] quantum non-demolition measurements,[18–20] nuclear magnetic resonance quadrupolar system,[21] and a standing-wave optical lattice.[22]

However, in experiments, the generation of spin squeezing is quite challenging due to the decoherence effects. The vacancy centers[23] may be promising candidates to generate spin squeezing because of their versatile quantum properties. A number of schemes to generate spin squeezed states were proposed recently in nitrogen-vacancy (NV) center systerms.[3,24–28] According to recent studies, silicon vacant color centers (SiV) are more superior than other vacant centers.[29–32] SiV center is formed by a silicon atom replacing a carbon atom in the diamond and then trapping a hole around it.[33] Since the atoms do not bond with the vacancy, it makes the electrons extremely sensitive to small changes in the electrical, magnetic, and optical properties in the surrounding environment[4,29,31,34] and is often used in the related research of spin-mechanical hybrid devices.[35] The neutral SiV in diamond is a candidate material for quantum network due to optical properties and long spin coherent time.[36] Besides, negatively charged SiV, which has good spectral characteristics and prepares spin states easily, is used in quantum communication, quantum information, and sensor areas.[31,36–39] Therefore, spin squeezed states in SiV systems may play an important role in the progress of science and technology.

In this paper, we propose an effective scheme to prepare the spin squeezed states by coupling SiV centers into one-dimensional diamond waveguides.[35,40–42] We derive the evolutions of spin squeezing in this system. The performance of spin squeezing with the spin numbers, the microwave field and other related parameters are studied. The results show that the perfect spin squeezing can be created even in the presence of spin relaxation induced by mechanical dissipation. The arrangement of this paper is as follows. We propose the model under study and give a brief explanation in Section 2. Then, we derive the Hamiltonian of the whole system and its complete dynamic description. The spin squeezing of the scheme is numerically studied in Section 3. We summarize this work

*Project supported by the National Natural Science Foundation of China (Grant No. 11664029) and the Inner Mongolia Natural Science Foundation, China (Grant No. 2021MS01012).

†Corresponding author. E-mail: myh_dlut@126.com
‡Corresponding author. E-mail: yusui.chen@nyit.edu

© 2021 Chinese Physical Society and IOP Publishing Ltd

and draw conclusions in Section 4. The mean values of the relevant mechanical quantities are presented in Appendix A.

2. The model and master equation

The theoretical model is shown in the Fig. 1(a), where N SiV centers are uniformly arranged in a one-dimensional diamond waveguide. Due to SiV orbital states' inversion symmetry, the lack of the permanent magnetic moment for an electric couple decreases its response to local environmental charge fluctuations.[5,43,44] The optical ground state contains two distinct electronic configurations corresponding to the presence of the unpaired hole in one of the even-parity orbitals e_{g+} and e_{g-}. Physically, the two branches in the optical ground state correspond to the occupation. In a zero magnetic field, the degeneracy of these orbitals is broken by spin–orbit coupling leading to frequency splitting $\Delta = 2\pi \times 46$ GHZ.[38] Upon applying a magnetic field, the degeneracy between the spin–orbit eigenstates is further broken and split into two sublevels within each orbital branch corresponding to different spin states of the unpaired hole. Therefore, SiV centers are equivalent to the four-level systems, consisting of two doublets. The energy gap is determined by spin–orbit interactions and a weak Jahn–Teller effect to the item, as shown in Fig. 1(b). $|e_{g+}\downarrow\rangle \sim |1\rangle$, $|e_{g-}\uparrow\rangle \sim |2\rangle$, $|e_{g-}\downarrow\rangle \sim |3\rangle$ and $|e_{g+}\uparrow\rangle \sim |4\rangle$.

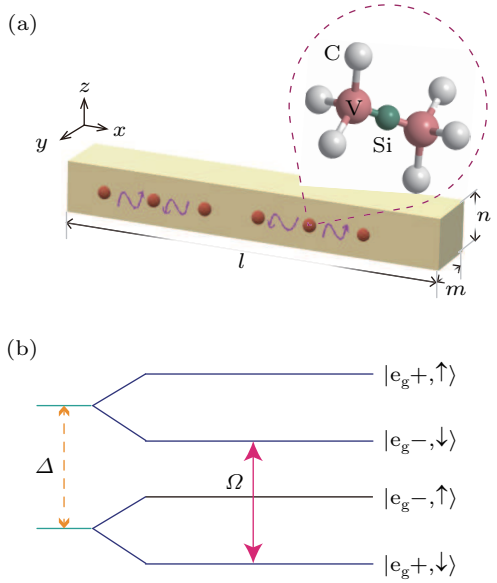


Fig. 1. (a) The SiV color centers are uniformly placed in a one-dimensional diamond waveguide. The length, width and height of the waveguide are l, m and n, respectively, with $l \gg \{m,n\}$. (b) Splitting of energy levels in a magnetic field B_z.

The spin mechanical dynamics for the system can be described by Hamiltonian[33]

$$\hat{H} = \hat{H}_{\rm siv} + \hat{H}_{\rm int} + \hat{H}_{\rm m}, \tag{1}$$

where the first term in $\hat{H}$ is the dynamic description of N SiV color centers in the waveguide, the second term is the interaction between SiV centers and the one-dimensional diamond waveguide, and the last term is the Hamiltonian of the one-dimensional diamond waveguide. These three terms are denoted by

$$\begin{aligned}
\hat{H}_{\rm siv} &= \omega_{\rm B}|2\rangle\langle 2| + \Delta|3\rangle\langle 3| + (\omega_{\rm B}+\Delta)|4\rangle\langle 4| \\
&\quad + \frac{1}{2}[\Omega e^{-i\omega_{\rm d} t} e^{i\theta_{\rm l}}(|2\rangle\langle 3| + |1\rangle\langle 4|) + {\rm H.C.}], \\
\hat{H}_{\rm int} &= \sum_{n=1}^{N} g[\hat{b}(|3\rangle_n\langle 1| + |4\rangle_n\langle 2|) + (|1\rangle_n\langle 3| + |2\rangle_n\langle 4|)\hat{b}^\dagger], \\
\hat{H}_{\rm m} &= \omega_{\rm m}\hat{b}^\dagger\hat{b},
\end{aligned} \tag{2}$$

where $\omega_{\rm B}$ is the Zeeman energy, $g \simeq (d/v_{\rm l})\sqrt{(\hbar\omega_{\rm m})/(2\rho lmn)}$ is SiV center's the spin–phonon coupling constant, $d/2\pi \sim 1000$ THz is the strain sensitivity, $\omega_{\rm m} \sim 2\pi \times 46$ GHz is the mechanical frequency, and Δ is the detuning of the spin–phonon couplings. The group velocities for a longitudinal squeezing is $v_{\rm l} = 1.7 \times 10^4$ m/s and a transverse flexural mode is $v_{\rm t} = 0.73 \times 10^4$ m/s.[33,45] $\hat{b}$ and $\hat{b}^\dagger$ are annihilation and creation operators of the oscillating mode, respectively. In this paper, to obtain spin squeezed states, we consider the case $B_z \to 0$. Then SiV center spins can be simplified to a two-level system denoted as $|1^j\rangle$ and $|3^j\rangle$, and the spin-conserving lowering operator is simplified to $\hat{\sigma}_-^j \to |1^j\rangle\langle 3^j|$. The collective spin operators are defined as $\hat{J}_- = (\hat{J}_+)^\dagger = \sum_{j=1}^{N}|1^j\rangle\langle 3^j|$, $\hat{J}_x = (1/2)(\hat{J}_- + \hat{J}_+)$, and $\hat{J}_y = (i/2)(\hat{J}_- - \hat{J}_+)$, satisfying

$$\begin{aligned}
[\hat{J}_\alpha, \hat{J}_\beta] &= i\varepsilon_{\alpha\beta\gamma}\hat{J}_\gamma, \\
[\hat{J}_+, \hat{J}_-] &= 2\hat{J}_z, \\
[\hat{J}_z, \hat{J}_\pm] &= \pm\hat{J}_\pm,
\end{aligned} \tag{3}$$

with $\varepsilon_{\alpha\beta\gamma}$ the Levi–Civita symbol, and the Hamiltonian then can be represented as

$$\hat{H} = \omega_{\rm m}\hat{b}^\dagger\hat{b} + \omega_{\rm s}\hat{J}_z + g_{\rm e}(\hat{b}^\dagger\hat{J}_- + \hat{b}\hat{J}_+), \tag{4}$$

where $g_{\rm e} \simeq \sqrt{N}g$ is the collective coupling strength, and $\omega_{\rm s} \sim D \approx 2\pi \times 46$ GHz is the resonance frequency of SiV spins. In the large detuning condition $g_{\rm e} \ll \Delta = |\omega_{\rm s} - \omega_{\rm m}|$ and in a frame rotating at the mechanical frequency $\omega_{\rm m}$, by performing the Frölich–Nakajima transform $\hat{H}_{\rm eff} = e^{-R}\hat{H}e^{R}$ to $\hat{H}_{\rm I} = \Delta\hat{J}_z + g_{\rm e}(\hat{b}^\dagger\hat{J}_- + \hat{b}^\dagger\hat{J}_+)$, we obtain an effective Hamiltonian[33]

$$\hat{H}_{\rm eff} \simeq (\Delta + \lambda + 2\lambda\hat{b}^\dagger\hat{b})\hat{J}_z - \lambda\hat{J}_z^2, \tag{5}$$

where $\lambda = g_{\rm e}^2/\Delta$ is the coupling strength of the effective spin-spin interactions. Adding the microwave field between this two-level system, Hamiltonian of the whole system can be written as

$$\hat{H}_{\rm eff} \simeq (\Delta + \lambda + 2\lambda\hat{b}^\dagger\hat{b})\hat{J}_z - \lambda\hat{J}_z^2 + \Omega(\hat{J}_+ + \hat{J}_-), \tag{6}$$

where Ω is effective Rabi frequency. For convenience, we set $a = \Delta + \lambda + 2\lambda\hat{b}^\dagger\hat{b}$, $b = \lambda$ and $c = 2\Omega$. Then, the effective Hamiltonian can be written in the following form:

$$\hat{H}_{\rm eff} \simeq a\hat{J}_z - b\hat{J}_z^2 + c\hat{J}_x. \tag{7}$$

Since the environment will inevitably influence the system, to fit the actual situation, we consider the decoherence and spin relaxation of the system and write the Markovian Lindblad master equation as

$$\frac{\mathrm{d}\hat{\rho}(t)}{\mathrm{d}t} = -\mathrm{i}[\hat{H}_{\mathrm{eff}},\hat{\rho}]+\gamma_{\mathrm{s}}\mathcal{D}(\hat{J}_z) +(n_{\mathrm{th}}+1)\Gamma_{\mathrm{m}}\mathcal{D}(\hat{J}_-)+n_{\mathrm{th}}\Gamma_{\mathrm{m}}\mathcal{D}(\hat{J}_+), \quad (8)$$

where $n_{\mathrm{th}}=(\mathrm{e}^{\hbar\omega_{\mathrm{m}}/k_{\mathrm{B}}T}-1)^{-1}$ is the number of thermal phonon at the environment temperature T with Boltzmann constant k_{B}. The super operator $\mathcal{D}$ satisfies $\mathcal{D}(\hat{A})\hat{\rho}=\hat{A}\hat{\rho}\hat{A}^{\dagger}-(1/2)\hat{A}^{\dagger}\hat{A}\hat{\rho}-(1/2)\hat{\rho}\hat{A}^{\dagger}\hat{A}$ for a given operator $\hat{A}$. Collective spin relaxation induced by mechanical dissipation is described in the last two terms with $\Gamma_{\mathrm{m}}=\gamma_{\mathrm{m}}g_{\mathrm{e}}^2/\Delta^2$ with γ_{m} the decay of mechanical modes. We will demonstrate that the spin squeezing will survive under such dissipative conditions.

3. Analysis of spin squeezing

To create spin squeezed state, we initially prepare the SiV ensemble in a coherent spin state along the x-axis of the Bloch sphere. Thus the initial conditions are $\langle J_z\rangle=0$, $\langle J_z^2\rangle=J/2$, $\langle J_-\rangle=\langle J_+\rangle=J$, $\langle J_-^2\rangle=\langle J_+^2\rangle=J(J-(1/2))$ and $\langle J_zJ_-\rangle=\langle J_+J_z\rangle=-J/2$. We employ the spin squeezing parameter ξ^2 to ascertain spin squeezing,[1,2,9,46] which can be defined as

$$\xi^2=\frac{N\langle\Delta J_{\mathrm{min}}^2\rangle}{\langle J_x\rangle^2}, \quad (9)$$

where

$$\langle\Delta J_{\mathrm{min}}^2\rangle = \frac{1}{2}\left(\langle J_y^2+J_z^2\rangle-\sqrt{\left(\langle J_y^2-J_z^2\rangle\right)^2+4\langle J_yJ_z\rangle_{\mathrm{ss}}^2}\right), \quad (10)$$

$$\langle\hat{J}_y\hat{J}_z\rangle_{\mathrm{ss}} = \frac{1}{2}\langle\hat{J}_y\hat{J}_z+\hat{J}_z\hat{J}_y\rangle = \frac{1}{4\mathrm{i}}\langle 2J_+J_z-2J_-J_z+J_++J_-\rangle. \quad (11)$$

The detailed calculation of the mean values used in ξ^2 is shown in Appendix A. When the spin squeezing parameter is equal to 1, it corresponds to the coherent state; When the parameter satisfies $\xi^2<1$, it is a spin squeezed state.

Firstly, we consider the time evolution of spin squeezing with different spin number N when the microwave field is absent ($c=0$). According to the simulation results in Fig. 2(a), the degree of spin squeezing becomes strong as the spin number N increases. However, the change will not be obvious when N reaches 300. This kind of spin squeezing can occur with the absence of microwaves, which was confirmed in previous studies.[35] Then, we pay attention to the case in the presence of a microwave field ($c\neq 0$). As shown in Fig. 2(b), the existence of a microwave field has a noticeable influence on the spin squeezing of the system. We observe that the degree of spin squeezing mounts significantly with varying growth values of the enhancive microwave field c ($c=2\Omega_{\mathrm{eff}}$). Moreover, the simulation results show that long time and high-intensity spin squeezing appear with the increase of the ratio c/a, until $c/a=1$. This is because the spin direction of SiV centers changes under the action of an external microwave field, which results in a stronger coupling effect and a higher degree of squeezing. Therefore, it is more significant that the desired spin squeezing effect can be achieved by applying and adjusting the external microwave field's intensity and direction. In particular, due to the $D_{3\mathrm{d}}$ anti-symmetry structure of SiV, we can reasonably adjust the magnetic field direction according to the symmetry axis of C_3.[23]

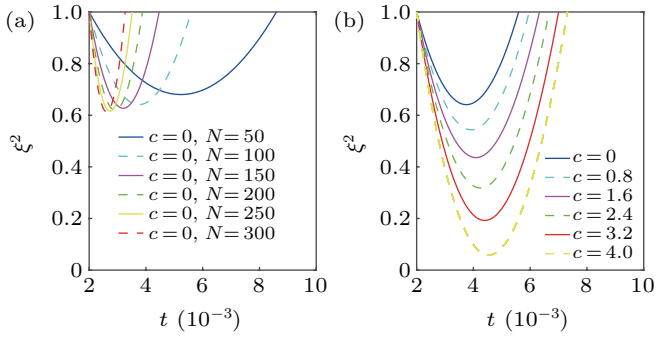


Fig. 2. Time evolution of spin squeezing parameter ξ^2 with (a) different spin number N and (b) different value of microwave field c. The parameters are (a) $a=b=4$, $c=0$, $n_{\mathrm{th}}=100$, $\Gamma_{\mathrm{m}}=0.05$ and $\gamma_{\mathrm{s}}=0.1$ with different spin number ($N=50$, 100, 150, 200, 250, 300 for the solid blue line, dashed cyan line, solid magenta line, dashed green line, solid yellow line and dashed red line, respectively); (b) $N=100$, $a=b=4$, $\Gamma_{\mathrm{m}}=0.05$ and $\gamma_{\mathrm{s}}=0.1$ with different value of microwave field ($c=0$, 0.8, 1.6, 2,4, 3.2, 4.0 for the solid blue line, dashed cyan line, solid magenta line, dashed green line, solid red line and dashed yellow line, respectively).

Next, let's focus on the related parameters in the effective Hamiltonian for Eq. (7). In Fig. 3, we plot the time evolution of the spin squeezing parameter ξ^2 with different a and b. As shown in Fig. 3(a), long time and high-intensity spin squeezing can be obtained with the downtrend of ratio a/c, that is, the preferable spin squeezing states will be obtained with the smaller ratio a/c. However, the ratio a/c should not be less than 1, because the degree of spin squeezing does not change significantly in this case. Figure 3(b) shows that the period of spin squeezing decreases, the maximum spin squeezing increases corresponding to the minimum value of ξ, as b/c decreases.

Inspired by the results in Figs. 2 and 3, we are aware of the strength and survival time of spin squeezing reach optimal values when $a=b=c$. In Fig. 4(a), we plot the time evolutions of spin squeezing with different numbers of SiV centers for a finite temperature. The results show that the relatively large spin numbers not only increase the maximum spin squeezing but also prolong the survival time of the whole process because the degree of spin squeezing is positively correlated with the number of particles N. The more SiV centers in a one-dimensional quasi-diamond waveguide, the stronger coupling

between different SiV centers and the easier spin squeezing generating. If the number of spin N continues to increase, ξ^2 will approach 0. It indicates that the squeezing amount can be increased indefinitely by increasing the total number of SiV centers. However, the more SiV centers there are, the higher loss rate will be increased in the experiment.

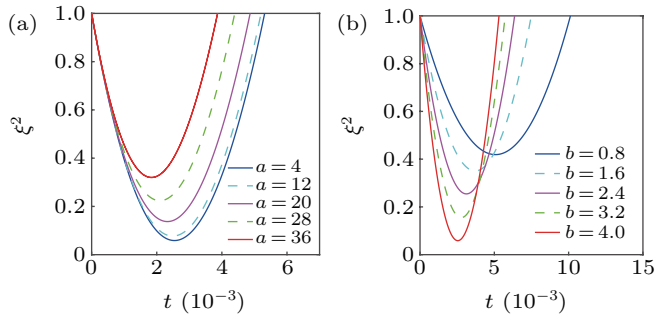


Fig. 3. Time evolution of spin squeezing parameter ξ^2 with (a) different value of a and (b) different value of b. The parameters are (a) $b=c=4$, $n_{\rm th}=100$, $N=100$, $\gamma_{\rm s}=0.1$, and $\Gamma_{\rm m}=0.05$ with different a ($a=4,12,20,28,36$ for the solid blue line, dashed cyan line, solid magenta line, dashed green line and solid red line, respectively); (b) $a=c=4$, $n_{\rm th}=100$, $N=100$, $\gamma_{\rm s}=0.1$, and $\Gamma_{\rm m}=0.05$ with different b ($b=0,0.8,1.6,2,4,3.2,4.0$ for the solid blue line, dashed cyan line, solid magenta line, dashed green line and solid red line, respectively).

Also, we need to consider the effect of the thermal phonon number related to the selection of ambient temperature on the system. In Fig. 4(b), the high-intensity spin squeezing with a longer period will be obtained with the decrease of the thermal phonon number or the decrease of the environment temperature. The reason is that the decoherence effect will be weakened with the decrease of temperature. So the coupling between spins will be enhanced, and the stronger spin squeezing will be reflected simultaneously.

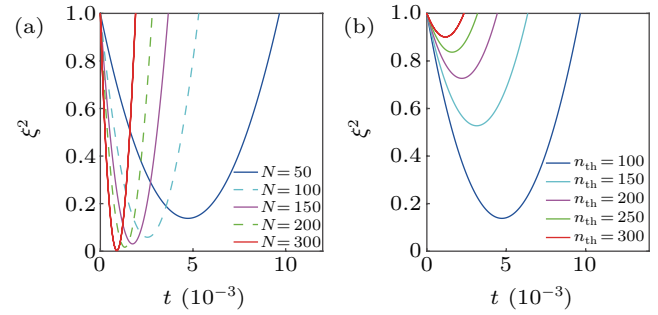


Fig. 4. (a) Time evolution of spin squeezing parameter ξ^2 with different spin number N. The parameters are $a=b=c=4$, $n_{\rm th}=100$, $\Gamma_{\rm m}=0.05$, $\gamma_{\rm s}=0.1$ with different spin number N ($N=50,100,150,200,300$ for the solid blue line, dashed cyan line, solid magenta line, dashed green line and solid red line, respectively). (b) Time evolution of spin squeezing parameter ξ^2 with different thermal phonon number $n_{\rm th}$. The parameters are $N=50$, $a=b=c=4$, $\Gamma_{\rm m}=0.05$ and $\gamma_{\rm s}=0.1$ with different thermal phonon number $n_{\rm th}$ ($n_{\rm th}=100,150,200,250,300$ for the solid blue line, solid green line, solid magenta line, solid cyan line and solid red line, respectively).

Since the system inevitably interacts with the environment, we need to consider the effect of decoherence on the system. Based on a complete description of the dynamic evolution of the system, the influences of the dephasing ($\gamma_{\rm s}$) of the SiV spins, and the decay of the mechanical modes ($\Gamma_{\rm m}$) on spin squeezing are analyzed respectively, as shown in Fig. 5. As we would expect, the time range of spin squeezing may be prolonged as the decay rate $\Gamma_{\rm m}$ decreases in Fig. 5(a). The weaker of the decay rates are, the longer the system's dynamics will maintain. Moreover, by choosing different dephasing ($\gamma_{\rm s}$) in Fig. 5(b), it shows that the time range and spins squeezing degree almost remain the same. This is because the lower dephasing ($\gamma_{\rm s}$), the less affected of the system, and the trend of squeezing time and squeezing degree are increasing. As such, to achieve the maximum spin squeezing, the dephasing ($\gamma_{\rm s}$) of the SiV spins and the decay of the mechanical modes should be as small as possible.

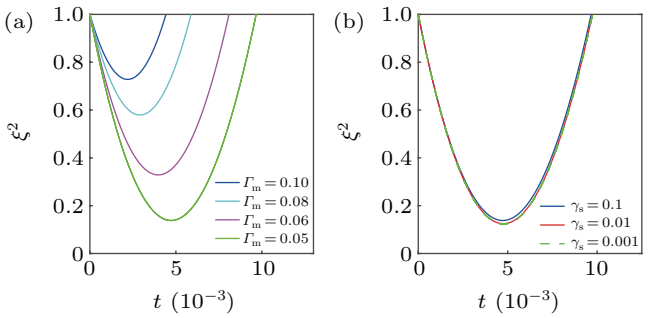


Fig. 5. Time evolution of spin squeezing parameter ξ^2 with (a) different value of effective mechanical decay rate $\Gamma_{\rm m}$ and (b) different value of spin dephasing rate $\gamma_{\rm s}$. The parameters are (a) $a=b=c=4$, $n_{\rm th}=100$, $N=50$, $\gamma_{\rm s}=0.1$ with different effective mechanical decay rate $\Gamma_{\rm m}$ ($\Gamma_{\rm m}=0.1$, 0.08, 0.06, 0.05 for the solid blue line, solid cyan line, solid magenta line and solid green line, respectively); (b) $a=b=c=4$, $n_{\rm th}=100$, $N=50$, $\Gamma_{\rm m}=0.05$ with different spin dephasing rate $\gamma_{\rm s}$ ($\gamma_{\rm s}=0.1$, 0.01, 0.001 for the solid blue line, solid red line and dashed green line, respectively).

4. Conclusion

One major advantage of building this kind of quantum device with SiV center rather than other solid-state systems is that SiV systems are typically more easily integrated into nanofabricated electrical and optical structures.[47,48] For example, a NV center in a diamond causes coupling to nearby electric field noise, which shifts its optical transition frequency as a function of time. However, SiV center is immune to this spectral diffusion to first order by its inversion symmetry and undoubtedly becomes an ideal candidate for integration into diamond waveguides. Another advantage is the excellent optical coherence property for SiV centers. We can characterize the optical coherence properties of SiV centers in nanostructures by photoluminescence excitation spectroscopy.[47] SiV centers have narrow transitions with $\Gamma_{\rm n}/2\pi=410\pm160$ MHz, which is about 4 times than the lifetime limited linewidth $\gamma/2\pi=94$ MHz. The ratios $\Gamma_{\rm n}/\gamma$ for SiV centers are much lower than the values for NV centers $\Gamma_{\rm n}/\gamma\gtrsim100$–$200$.[47]

Moreover, when SiV centers are coupled to diamond waveguide, we need to choose the appropriate waveguide dimensions and set the distance $L=a\sqrt{\alpha/(\Omega-\omega_0)}$[33] between the adjacent SiV centers reasonably according to the actual situation. The preparation of spin squeezing efficiency

and the performance of the system will be impacted due to the distance between the adjacent SiV centers in the case of decoherence. In the above parameters, α is a parameter characterizing the band curvature, and a is the lattice constant. We can choose the model's experimental values of the parameter $l \sim 20\ \mu\text{m}$, $m \sim 0.1\ \mu\text{m}$, $n \sim 0.1\ \mu\text{m}$, $\rho = 3500\ \text{kg/m}^3$, the Poisson ratio $\nu = 0.2$ and the Young's modulus $E = 1050$ GPa,[33,45] then the coupling constant is $g \sim 3400$ kHz.

In summary, it is feasible to prepare spin squeezing by coupling SiV centers into diamond waveguides. Under the condition of large detuning, to obtain high-strength spin squeezing with a long survivable time, we can decrease the environment temperature or increase the number of spin numbers. The application of the external microwave field effectively increases the degree of spin squeezing and prolongs the duration of the spin squeezing state. Furthermore, the stronger the degree of spin squeezing, the more difficult it is to maintain spin squeezing in the decoherence environment, which is expressed as Γ_{m} in the theoretical study. Therefore, the influence of decoherence on the system should be minimized. In practice, we can reduce the effect of decoherence on the system by improving the quality and purity of the materials.

Appendix A: Expectation of collective operators with time evolution

In this part, we calculate the average values that enter the variance of Eq. (9). It is well know that the evolution of the spin average for an operator $\hat{A}$ can be described by $\text{d}\langle\hat{A}\rangle/\text{d}t = \text{Tr}(\hat{A}\dot{\rho})$, as is shown in the following equation:

$$\begin{aligned}\frac{\text{d}\langle\hat{A}\rangle}{\text{d}t} &= -\text{i}\left\langle\left[\hat{A},\hat{H}_{\text{eff}}\right]\right\rangle + \frac{1}{2}\gamma_{\text{s}}\left(\left\langle\left[\hat{J}_z,\hat{A}\right]\hat{J}_z\right\rangle + \left\langle\hat{J}_z\left[\hat{A},\hat{J}_z\right]\right\rangle\right)\\ &+\frac{1}{2}\Gamma_{\text{m}}\left(n_{\text{th}}+1\right)\left(\left\langle\left[\hat{J}_+,\hat{A}\right]\hat{J}_-\right\rangle + \left\langle\hat{J}_+\left[\hat{A},\hat{J}_-\right]\right\rangle\right)\\ &+\frac{1}{2}\Gamma_{\text{m}}n_{\text{th}}\left(\left\langle\hat{J}_-\left[\hat{A},\hat{J}_+\right]\right\rangle + \left\langle\left[\hat{J}_-,\hat{A}\right]\hat{J}_+\right\rangle\right). \qquad \text{(A1)}\end{aligned}$$

With the help of Eq. (A1), we can obtain the following equations easily:

$$\begin{aligned}\frac{\text{d}\langle\hat{J}_z\rangle}{\text{d}t} &= \frac{c}{2\text{i}}\left\langle\hat{J}_+ - \hat{J}_-\right\rangle - \Gamma_{\text{m}}\left(n_{\text{th}}+1\right)\left\langle\hat{J}_+\hat{J}_-\right\rangle\\ &+\Gamma_{\text{m}}n_{\text{th}}\left\langle\hat{J}_-\hat{J}_+\right\rangle, \qquad \text{(A2)}\\ \frac{\text{d}\langle\hat{J}_-\rangle}{\text{d}t} &= -\text{i}a\left\langle\hat{J}_-\right\rangle + \text{i}c\left\langle\hat{J}_z\right\rangle + \text{i}b\left[2\left\langle\hat{J}_z\hat{J}_-\right\rangle + \left\langle\hat{J}_-\right\rangle\right]\\ &-\frac{1}{2}\gamma_{\text{s}}\left\langle\hat{J}_-\right\rangle + \Gamma_{\text{m}}\left(n_{\text{th}}+1\right)\left\langle\hat{J}_z\hat{J}_-\right\rangle\\ &-\Gamma_{\text{m}}n_{\text{th}}\left(\left\langle\hat{J}_z\hat{J}_-\right\rangle + \left\langle\hat{J}_-\right\rangle\right), \qquad \text{(A3)}\\ \frac{\text{d}\langle\hat{J}_z^2\rangle}{\text{d}t} &= \frac{c}{2\text{i}}\left[-2\left\langle\hat{J}_z\hat{J}_-\right\rangle - \left\langle\hat{J}_-\right\rangle + 2\left\langle\hat{J}_+\hat{J}_z\right\rangle + \left\langle\hat{J}_+\right\rangle\right]\\ &+\Gamma_{\text{m}}\left(n_{\text{th}}+1\right)\left[-2J\left(J+1\right)\left\langle\hat{J}_z\right\rangle + 2\left\langle\hat{J}_z^3\right\rangle\right.\\ &\left.-3\left\langle\hat{J}_z^2\right\rangle + \left\langle\hat{J}_z\right\rangle + J\left(J+1\right)\right]\\ &+\Gamma_{\text{m}}n_{\text{th}}\left[2J\left(J+1\right)\left\langle\hat{J}_z\right\rangle - 2\left\langle\hat{J}_z^3\right\rangle\right.\\ &\left.-3\left\langle\hat{J}_z^2\right\rangle - \left\langle\hat{J}_z\right\rangle + J\left(J+1\right)\right], \qquad \text{(A4)}\\ \frac{\text{d}\langle\hat{J}_-^2\rangle}{\text{d}t} &= -2\text{i}a\left\langle\hat{J}_-^2\right\rangle + \text{i}b\left(2\left\langle\hat{J}_z\hat{J}_-^2\right\rangle + 2\left\langle\hat{J}_-^2\hat{J}_z\right\rangle\right)\\ &+\text{i}c\left(2\left\langle\hat{J}_z\hat{J}_-\right\rangle + \left\langle\hat{J}_-\right\rangle\right) - 2\gamma_{\text{s}}\left\langle\hat{J}_-^2\right\rangle\\ &+\Gamma_{\text{m}}\left(n_{\text{th}}+1\right)\left(2\left\langle\hat{J}_z\hat{J}_-^2\right\rangle + \left\langle\hat{J}_-^2\right\rangle\right)\\ &-\Gamma_{\text{m}}n_{\text{th}}\left(2\left\langle\hat{J}_z\hat{J}_-^2\right\rangle + 3\left\langle\hat{J}_-^2\right\rangle\right), \qquad \text{(A5)}\\ \frac{\text{d}\langle\hat{J}_z\hat{J}_-\rangle}{\text{d}t} &= -\text{i}a\left\langle\hat{J}_z\hat{J}_-\right\rangle + 2\text{i}b\left\langle\hat{J}_z^2\hat{J}_-\right\rangle + \text{i}b\left\langle\hat{J}_z\hat{J}_-\right\rangle\\ &+\frac{c}{2\text{i}}\left(\left\langle\hat{J}_+\hat{J}_-\right\rangle - \left\langle\hat{J}_-^2\right\rangle\right) - \frac{1}{2}\gamma_{\text{s}}\left\langle\hat{J}_z\hat{J}_-\right\rangle\\ &+\Gamma_{\text{m}}\left(n_{\text{th}}+1\right)\left[-J\left(J+1\right)\left\langle\hat{J}_-\right\rangle\right.\\ &\left.+2\left\langle\hat{J}_z^2\hat{J}_-\right\rangle - \left\langle\hat{J}_z\hat{J}_-\right\rangle\right]\\ &+\Gamma_{\text{m}}n_{\text{th}}\left[J\left(J+1\right)\left\langle\hat{J}_-\right\rangle - 2\left\langle\hat{J}_z^2\hat{J}_-\right\rangle\right.\\ &\left.-4\left\langle\hat{J}_z\hat{J}_-\right\rangle - 2\left\langle\hat{J}_-\right\rangle\right]. \qquad \text{(A6)}\end{aligned}$$

References

[1] Kitagawa M and Ueda M 1993 *Phys. Rev. A* **47** 5138
[2] Ma J, Wang X, Sun C P and Nori F 2011 *Phys. Rep.* **509** 89
[3] Bennett S, Yao N Y, Otterbach J, Zoller P, Rabl P and Lukin M D 2013 *Phys. Rev. Lett.* **110** 156402
[4] Chen D, Zheludev N and Gao W B 2020 *Adv. Quantum Technol.* **3** 1900069
[5] Nguyen C, Sukachev D, Bhaskar M, Machielse B, Levonian D, Knall E, Stroganov P, Chia C, Burek M and Riedinger R 2019 *Phys. Rev. B* **100** 165428
[6] Vitagliano G, Hyllus P, Egusquiza I L and Tóth G 2011 *Phys. Rev. Lett.* **107** 240502
[7] Sau J D, Leslie S R, Cohen M L and Stamper-Kurn D M 2010 *New J. Phys* **12** 085011
[8] Tóth G, Knapp C, Gühne O, Briegel H J, Tóth G, Knapp C, Gühne O and Briegel H J 2009 *Phys. Rev. A* **79** 042334
[9] Wineland D J, Bollinger J J, Itano W M, Moore F and Heinzen D 1992 *Phys. Rev. A* **46** R6797
[10] Laudat T, Dugrain V, Mazzoni T, Huang M Z, Alzar C L G, Sinatra A, Rosenbusch P and Reichel J 2018 *New J. Phys.* **20** 073018
[11] Jo G-B, Shin Y, Will S, Pasquini T, Saba M, Ketterle W, Pritchard D E, Vengalattore M and Prentiss M 2007 *Phys. Rev. Lett.* **98** 030407
[12] Li W, Tuchman A K, Chien H C and Kasevich M A 2007 *Phys. Rev. Lett.* **98** 040402
[13] Hosten O, Engelsen N J, Krishnakumar R and Kasevich M A 2016 *Nature* **529** 505
[14] Cox K C, Greve G P, Weiner J M and Thompson J K 2016 *Phys. Rev. Lett.* **116** 093602
[15] Mertens S and Moore C 2018 *Phys. Rev. E* **98** 022120
[16] Sofiev M, Berger U, Prank M, Vira J, Arteta J, Belmonte J, Bergmann K C, Chéroux F, Elbern H and Friese E 2015 *Atmos. Chem. Phys.* **15** 8115
[17] Vengalattore M, Higbie J, Leslie S, Guzman J, Sadler L and Stamper-Kurn D 2007 *Phys. Rev. Lett.* **98** 200801
[18] Johnson B, Reed M, Houck A A, Schuster D, Bishop L S, Ginossar E, Gambetta J, DiCarlo L, Frunzio L and Girvin S 2010 *Nat. Phys.* **6** 663
[19] Saffman M, Oblak D, Appel J and Polzik E 2009 *Phys. Rev. A* **79** 023831
[20] Shah V, Vasilakis G and Romalis M 2010 *Phys. Rev. Lett.* **104** 013601
[21] Auccaise R, Araujo-Ferreira A, Sarthour R, Oliveira I, Bonagamba T J and Roditi I 2015 *Phys. Rev. Lett.* **114** 043604
[22] Lewis-Swan R J, Norcia M A, Cline J R, Thompson J K and Rey A M 2018 *Phys. Rev. Lett.* **121** 070403
[23] Bradac C, Gao W, Forneris J, Trusheim M E and Aharonovich I 2019 *Nat. Commun.* **10** 1
[24] Ma Y H, Zhang X F, Song J and Wu E 2016 *Ann. Phys.* **369** 36

[25] Dooley S, Yukawa E, Matsuzaki Y, Knee G C, Munro W J and Nemoto K 2016 *New J. Phys.* **18** 053011
[26] Ma Y H and Zhang X F 2014 *Phys. Rev. B* **89** 144113
[27] Ma Y H, Ding Q Z and Yu T 2020 *Phys. Rev. A* **101** 022327
[28] Xia K and Twamley J 2016 *Phys. Rev. B* **94** 205118
[29] Maity S, Shao L, Bogdanovi S, Meesala S, Sohn Y I, Sinclair N, Pingault B, Chalupnik M, Chia C and Zheng L 2020 *Nat. Commun.* **11** 1
[30] Lee D, Lee K W, Cady J V, Ovartchaiyapong P and Jayich A C B 2017 *J. Opt.* **19** 033001
[31] Becker J N and Becher C 2017 *Phys. Status Solidi A* **214** 1700586
[32] Lindner S, Bommer A, Muzha A, Krueger A, Gines L, Mandal S, Williams O, Londero E, Gali A and Becher C 2018 *New J. Phys.* **20** 115002
[33] Li P B, Li X X and Nori F 2019 arXiv:1901.04650
[34] Jahnke K D, Sipahigil A, Binder J M, Doherty M W, Metsch M, Rogers L J, Manson N B, Lukin M D and Jelezko F 2015 *New J. Phys.* **17** 043011
[35] Li B, Li X, Li P and Li T 2020 *Adv. Quantum Technol.* **3** 2000034
[36] Rose B C, Huang D, Zhang Z H, Stevenson P, Tyryshkin A M, Sangtawesin S, Srinivasan S, Loudin L, Markham M L and Edmonds A M 2018 *Science* **361** 60
[37] Sukachev D D, Sipahigil A, Nguyen C T, Bhaskar M K, Evans R E, Jelezko F and Lukin M D 2017 *Phys. Rev. Lett.* **119** 223602
[38] Meesala S, Sohn Y I, Pingault B, Shao L, Atikian H A, Holzgrafe J, Gündoan M, Stavrakas C, Sipahigil A and Chia C 2018 *Phys. Rev. B* **97** 205444
[39] Weinzetl C, Görlitz J, Becker J N, Walmsley I A, Poem E, Nunn J and Becher C 2019 *Phys. Rev. Lett.* **122** 063601
[40] Lemonde M A, Meesala S, Sipahigil A, Schuetz M, Lukin M, Loncar M and Rabl P 2018 *Phys. Rev. Lett.* **120** 213603
[41] Qiao Y F, Li H Z, Dong X L, Chen J Q, Zhou Y and Li P B 2020 *Phys. Rev. A* **101** 042313
[42] Song W, Yang W, An J and Feng M 2017 *Opt. Express* **25** 19226
[43] Bray K, Regan B, Trycz A, Previdi R, Seniutinas G, Ganesan K, Kianinia M, Kim S and Aharonovich I 2018 *ACS Photonics* **5** 4817
[44] Bhaskar M K, Sukachev D D, Sipahigil A, Evans R E, Burek M J, Nguyen C T, Rogers L J, Siyushev P, Metsch M H and Park H 2017 *Phys. Rev. Lett.* **118** 223603
[45] Golter D A, Oo T, Amezcua M, Lekavicius I, Stewart K A and Wang H 2016 *Phys. Rev. X* **6** 041060
[46] Jin G R, Liu Y C and Liu W M 2009 *New J. Phys.* **11** 073049
[47] Evans R E, Sipahigil A, Sukachev D D, Zibrov A S and Lukin M D 2016 *Phys. Rev. Applied* **5** 044010
[48] Ladd T D, Jelezko F, Laflamme R, Nakamura Y, Monroe C and O'Brien J L 2010 *Nature* **464** 45